ACS AuthorChoice

Article

pubs.acs.org/Biomac

Probing the Biomimetic Ice Nucleation Inhibition Activity of Poly(vinyl alcohol) and Comparison to Synthetic and Biological Polymers

Thomas Congdon, Bethany T. Dean, James Kasperczak-Wright, Caroline I. Biggs, Rebecca Notman, and Matthew I. Gibson*

Department of Chemistry, University of Warwick, Coventry, CV4 7AL, United Kingdom

Supporting Information

ABSTRACT: Nature has evolved many elegant solutions to enable life to flourish at low temperatures by either allowing (tolerance) or preventing (avoidance) ice formation. These processes are typically controlled by ice nucleating proteins or antifreeze proteins, which act to either promote nucleation, prevent nucleation or inhibit ice growth depending on the specific need, respectively. These proteins can be expensive and their mechanisms of action are not understood, limiting their translation, especially into biomedical cryopreservation applications. Here well-defined poly(vinyl alcohol), synthesized by RAFT/MADIX polymerization, is investigated for its ice nucleation inhibition (INI) activity, in contrast to its established ice growth inhibitory properties and compared to other synthetic polymers. It is shown that ice nucleation inhibition activity of PVA has a strong molecular weight dependence; polymers with a degree of polymerization below 200 being an effective inhibitor at just 1 mg.mL^{-1}. Other synthetic and natural polymers, both with and without hydroxyl-functional side chains, showed negligible activity, highlighting the unique ice/water interacting properties of PVA. These findings both aid our understanding of ice nucleation but demonstrate the potential of engineering synthetic polymers as new biomimetics to control ice formation/growth processes

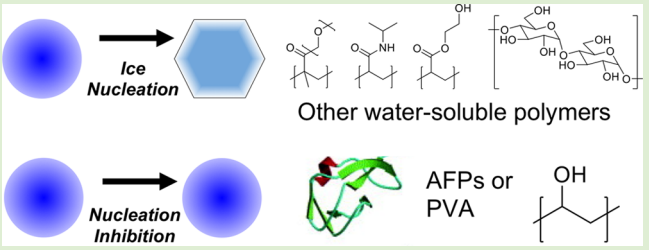

INTRODUCTION

Ice formation via heterogeneous nucleation is crucial in the context of atmospheric science,[1] cryopreservation,[2] cryomedicine,[3] cryosurgery,[4] and also food science.[5] The challenges in understanding, and in particular, predicting homogeneous and heterogeneous nucleation temperatures cannot be understated. For example, in the vitreous cryopreservation of cells and tissue for transplantation medicine, ice nucleation must be suppressed until the glass transition temperature is reached to ensure a glassy, rather than ice-rich phase.[6] In frozen foods, ice nucleation at relatively high temperatures generates larger ice particles than at lower temperatures. A difference in ice grain size, from 15 to 20 to 40 μm, will cause an unpalatable difference in the quality and taste of ice cream.[7]

While ice formation in water (freezing) is thermodynamically favorable at temperatures below 0 °C, there is a large kinetic barrier, resulting in the homogeneous (for ultrapure water) nucleation/freezing temperature being ∼−38 °C; the temperature when pure water spontaneously turns to ice at ambient pressure. In practice, the presence of impurities in water (dust, salts, bacteria, etc.) provide nucleation sites enabling nucleation to occur typically in the range of 0 to −20 °C in bulk samples. This complex phase behavior has proven to be challenging to understand, in part due to nucleation being a rare event, meaning computational modeling of the process is very challenging. The ability to predictably control ice nucleation temperature, however, would be technologically significant in applications ranging from the seeding of rain clouds to controlling ice build-up on wind turbines. Several inorganic minerals, such as kaolinite[8] and feldspar, have been shown to be very potent ice nucleators and may play a role in rain cloud formation via Saharan dust clouds.[9,10]

A large range of ice nucleating proteins exist, both in anthropods[11] and on the surface of bacteria.[12] The plant pathogen *Pseudomonas syringae* is capable of inducing ice nucleation on the leaves of plants, promoting frost formation and releasing nutrients for the bacteria.[13] Antifreeze proteins, which are highly effective at inhibiting ice growth, display some weak nucleation inhibition,[14] believed to arise due to the interactions with ice nucleating proteins. Extracellular proteins known as ice nucleating proteins have found commercial use in snow making.[15] In contrast to the above, many extremophile organisms have evolved antifreeze (glyco)proteins (AF(G)Ps) to protect themselves from cold damage (in some cases in response to ice nucleating bacteria). While the primary roles of AF(G)Ps are to depress the equilibrium freezing point and inhibit ice recrystallization (growth/ripening), they also show complex behavior in ice nucleation, both promoting[16] and

Received: June 10, 2015
Revised: August 8, 2015
Published: August 10, 2015

DOI: 10.1021/acs.biomac.5b00774
Biomacromolecules 2015, 16, 2820−2826

inhibiting[17] dependent on the conditions.[18] Extremophiles will often exploit a range of these methods in parallel in order to survive.[19,20]

The major challenge with the study of AF(G)Ps and ice nucleating proteins is that they are synthetically challenging to access. Ben et al. have developed small molecule mimics of AF(G)Ps,[21,22] and Gibson et al. have shown that synthetic polymers can reproduce the ice recrystallization inhibition properties of AF(G)Ps, and applied this to nonvitreous cryopreservation, but far fewer examples exist of polymers with ice nucleation properties. Poly(vinyl alcohol) (PVA) is established as a highly potent inhibitor of ice growth in frozen and vitrified media,[23,24] and in particular lower molecular weight fractions display anomalously strong ice growth inhibition.[25] Polyglycerol has been reported to bind to and inhibit the ice nucleation activity of some proteins, and the combination of polyglycerol with poly(vinyl alcohol) was shown to be particularly effective for reducing ice formation in vitrified solutions.[26] The ice nucleation inhibition behavior of poly(vinylpyrrolidone) (PVP) and AF(G)P mixtures has been studied by Franks et al.,[27] but there remains a huge gap in the understanding of the design rules for the synthesis of ice nucleation inhibitors. PVA in combination with antifreeze proteins have been used to control ice crystal growth in ice slurries.[28] Lu et al. conducted detailed experiments into the inhibition of nucleation and growth of ice by PVA in vitrified solutions.[29] Nucleation inhibition activity using droplet freezing has been interrogated using a range of methods, including microfluidics,[30] suspension in oil,[31] or using electrodynamic balances.[32,33] Murray et al. have measured homogeneous and heterogeneous freezing of water using a hydrophobic substrate and an optical microscope,[34] and this method has also been used to examine the effect of surface topography on droplet nucleation.[35] Using a multipoint freezing assay, highly disperse, partly acetylated PVA has been shown to display ice nucleation inhibition activity.[16] Conversely, studies using commercial PVA (with no additional purification) at relatively high concentrations result in nucleation promotion rather than inhibition, showing the complexity of this process.[36,37]

While the above examples indicate that synthetic polymers could be useful tools to modulate and understand ice nucleation phenomena, all previous studies have been undertaken using either poorly defined PVA materials with high dispersities and unknown degrees of acetylation or using limited analytical methods that do not take into account the stochastic nature of ice nucleation (i.e., single measurements are not sufficient). In this work we employ RAFT/MADIX polymerization methodology to access a library of well-defined polymers to investigate how their structural features (molecular weight, side chains) influence nucleation as a first step to understanding and predicting new synthetic materials capable of reproducing extremophile function.

EXPERIMENTAL SECTION

Materials. Hydrophobic slides made of glass with a PTFE coating were purchased from Thermo Scientific, stored at 80 °C, and allowed to cool to ambient temperature prior to use. 4,4′-Azobis(4-cyanovaleric acid) (98%), dextran (9−10 kDa, 98%), hydrazine hydrate (80%) solution, *N*-hydroxyethyl acrylamide (97%), *N*-isopropylacrylamide (98%), poly(ethylene glycol) (M_n = 300), methyl ether methacrylate (99%), poly(vinyl alcohol) (75−100 kg mol^{-1}, 98%), poly(vinyl alcohol) (85−124 kg mol^{-1}, 98%), and vinyl acetate (99%) were purchased from Sigma-Aldrich. Hexane, methanol, and tetrahydrofuran were purchased from Fluka. *O*-Ethyl-*S*-1-phenyl carbonodithioate, 2-(pyridyldisulfanyl) ethyl 2-(dodecylthiocarbonothioylthio)-2-methylpropanoic acid, and poly(hydroxy ethyl acrylate) were synthesized using previously reported methods.[38,39]

Analytical and Physical Methods. ^{1}H and ^{13}C NMR spectra were recorded on Bruker DPX-300 and DPX-400 spectrometers using deuterated solvents purchased from Sigma-Aldrich. Chemical shifts are reported relative to residual nondeuterated solvent. Size exclusion chromatography (SEC) was used to examine and differentiate between the molecular weights and the dispersities of the synthesized polymers. The SEC analysis was performed on a Varian 390-LC MDS system equipped with a PL-AS RT/MT autosampler, a PL-gel 3 μm (50 × 7.5 mm) guard column, and two PL-gel 5 μm (300 × 7.5 mm) mixed-D columns held at 30 °C, and the instrument was equipped with a differential refractive index and a Shimadzu SPD-M20A diode array detector. Dimethylformamide (including 5 mM ammonium tetrafluoroborate) was used as the eluent at a flow rate of 1 mL min^{-1}. The THF SEC system comprised of a Varian 390-LC-Multi detector suite fitted with differential refractive index (DRI), light scattering (LS), and ultraviolet (UV) detectors equipped with a guard column (Varian Polymer Laboratories PLGel 5 μm, 50 × 7.5 mm) and two mixed D columns of the same type. The mobile phase was THF with 5% triethylamine (TEA) eluent at a flow of 1.0 mL/min, and samples were calibrated against Varian Polymer Laboratories EasiVials linear poly(styrene) and poly(methyl methacrylate) standards (162−2.4 × 10^5 g/mol) using Cirrus v3.3. The temperature of the ice and water droplets was controlled on a Linkam Biological Cryostage BCS196 with T95-Linkpad system controller equipped with a LNP95-liquid nitrogen cooling pump, using liquid nitrogen as the coolant (Linkam Scientific Instruments UK, Surrey, U.K.). Image and droplet monitoring was conducted using a Veho Discovery VMS-004 Deluxe USB microscope and Veho Microcapture software V 1.3.

Ice Nucleation Assay. This example is for a single polymer, but the same method was employed for each sample. PVA was dissolved in Milli-Q water over 24 h to give the desired concentration for the assay and to ensure complete solvation of the polymer. A total of 10 droplets (0.5 μL) were pipetted onto each slide, and the slide was placed inside a Linkham Scientific cryostage. The cryostage was rapidly cooled to 5 °C at a rate of 50 °C/min and then held at this temperature for 3 min to allow the temperature of the glass slide and droplets to equilibrate. The samples were then cooled from 5 °C to −40 °C at a rate of 2 °C/min. Ice nucleation was observed using a Veho Discovery VMS-004 Deluxe USB microscope and Veho Microcapture software V 1.3. The experiment was repeated with fresh droplets from the same stock solution until at least 20 droplet freezing temperatures were recorded.

Polymerization of Vinyl Acetate Using *O*-Ethyl-*S*-1-phenyl Carbonodithioate. As a representative example, *O*-ethyl-*S*-1-phenyl carbonodithioate (0.069 g, 0.35 mmol), vinyl acetate (4.67 g, 2.64 mmol), and ACVA (4,4′-azobis(4-cyanovaleric acid)) (0.005 g, 0.029 mmol) were added to a stoppered vial. The solution was thoroughly degassed under a flow of N_2 for 20 min, and the reaction mixture was then allowed to polymerize at 68 °C for typically 15 h. For short chain oligomers of PVAc, under these conditions, conversion proceeds at approximately 1% per minute, so for $PVAc_{13}$, the reaction was quenched using liquid nitrogen and exposing the vial to air after 10 min heating at 68 °C. The yellow solutions were then cooled to room temperature. Poly(vinyl acetate) was then recovered as a yellow sticky solid after precipitation into hexane. The hexane was decanted and the poly(vinyl acetate) was redissolved in THF, which was then concentrated in vacuo and thoroughly dried under vacuum at 40 °C for 24 h, forming an off-white solid. Representative characterization data for $PVAc_{183}$: ^{1}H NMR (400 MHz, $CDCl_3$): δ 4.61 (1H, br, C*H*O−CH_2), 1.74 (3H, br, CO−CH_3), 1.53 (2H, br, CH_2); M_n^{SEC}(THF) = 15800 Da, M_w/M_n = 1.16.

Hydrolysis of Poly(vinyl acetate) to Poly(vinyl alcohol). As a representative example, poly(vinyl acetate) (0.3 g, M_n 15800 g·mol^{-1}, $Đ$ = 1.16) was dissolved in a methanol (4 mL) in a round-bottom flask. Hydrazine hydrate solution (6 mL, 80% in water) was added, and the reaction mixture was stirred at 40 °C for 1 h until the solution became clear. The reaction mixture was then dialyzed using distilled water and poly(vinyl alcohol) was recovered as a spongy white solid by

DOI: 10.1021/acs.biomac.5b00774
Biomacromolecules 2015, 16, 2820−2826

Scheme 1. RAFT/MADIX Polymerization of Vinyl Acetate and Subsequent Hydrolysis to PVA Using Hydrazine Hydrate Solution

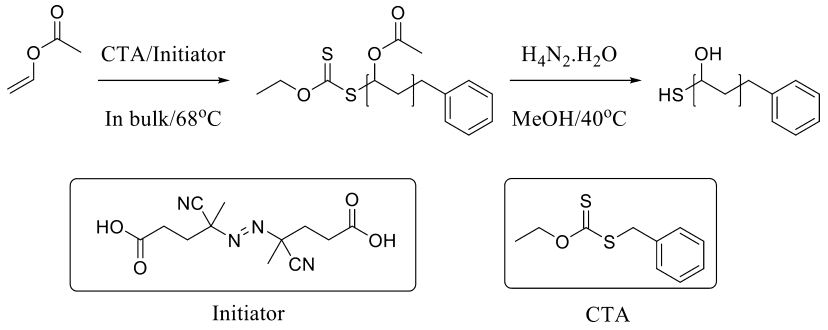

Table 1. PVA and PVA·PVAc Used in This Study

entry	[M]/[CTA]	M_n(Theo)[a] [g mol^{-1}]	M_n(SEC)[b] [g mol^{-1}]	$Đ$[b]	DP$_n$[c]	PVA[d]
PVAc$_{13}$	110	9500	1300	1.33	13	PVA$_{13}$
PVAc$_{73}$	70	6000	6300	1.11	73	PVA$_{73}$
PVAc$_{126}$	120	10300	10900	1.31	126	PVA$_{126}$
PVAc$_{183}$	155	13300	15800	1.16	183	PVA$_{183}$
PVAc$_{322}$	168	14500	27800	1.40	322	PVA$_{322}$
PVAc$_{366}$	395	34000	31500	1.48	366	PVA$_{366}$

[a]Theoretical number-average degree of polymerization, assuming 100% conversion. [b]Determined by SEC in THF using PMMA polymer standards. [c]Number-average degree of polymerization, determined from conversion of monomer to polymer by ^{1}H NMR. [d]Corresponding PVA prepared by complete hydrolysis of PVAc, determined by ^{1}H NMR.

freeze-drying the dialysis solution. For short chain PVA$_{10}$, the solution was diluted with water and washed with toluene (4 × 60 mL) to remove the organic solvents. The solution was then freeze-dried, and poly(vinyl alcohol) was recovered as a spongy white solid by freeze-drying the dialysis solution. Complete hydrolysis was confirmed by ^{1}H NMR. Representative characterization data for PVA$_{183}$: ^{1}H NMR (400 MHz, D_2O): δ 4.00 (1H, br, C*H*OH), 1.68−1.60 (2H, br, CH_2).

Polymerization of *N*-Isopropylacrylamide. Prepared according to a method adapted from literature.[40] *N*-isopropylacrylamide (1.00 g, 8.84 mmol), 2-(pyridyldisulfanyl) ethyl 2-(dodecylthiocarbonothioylthio)-2-methylpropanoic acid (43.0 mg, 0.118 mmol), and 4,4′-azobis(4-cyanovaleric acid) (6.60 mg, 23.6 μmol) were dissolved in methanol/toluene (1:1; 4 mL) in a glass vial containing a stir bar. The vial was degassed under a flow of nitrogen for 10 min and then heated at 70 °C for 1 h, after which the reaction mixture was opened to air and quenched in liquid nitrogen. The product was precipitated into cold diethyl ether and dried under vacuum to give a yellow solid. ^{1}H NMR (400 MHz, $CDCl_3$): δ 3.85−4.10 (1H, br, C*H*), 1.95−2.30 (2H, br, CH_2), 1.55−1.70 (1H, m, NC*H*), 1.0−1.20 (6H, d, CH_3). M_n^{SEC}(THF) = 9280 Da; M_w/M_n = 1.05.

Polymerization of Oligo(ethylene glycol) Methyl Ether Methacrylate. Poly(ethylene glycol) (M_n = 300) methyl ether methacrylate (2.00 g, 6.67 mmol), 2-(dodecylthiocarbonothioylthio)-2-methylpropanoic acid (3.74 mg, 10.3 μmol), and 4,4′-azobis(4-cyanovaleric acid). The vial was degassed under a flow of nitrogen for 10 min and then heated at 70 °C for 4 h. The reaction mixture was opened to air and quenched in liquid nitrogen. The product was precipitated into diethyl ether, isolated by centrifugation, and dried under vacuum overnight to give a waxy, yellow solid. Representative characterization data for p(OEGMA)$_{224}$. ^{1}H NMR (400 MHz, $CDCl_3$) δ 3.50−4.15 (16H, br d, PEG), 2.00 (3H, s, OCH_3), 1.55−1.90 (2H, m, CH_2), 0.75−1.75 (3H, m, CH_3). M_n^{SEC}(THF) = 175750 Da; M_w/M_n = 1.92.

General Procedure for Polymerization of *N*-Hydroxyethyl Acrylamide. 4,4-Azobis(4-cyanovaleric acid) (5 mg, 0.018 mmol), 2-(dodecylthiocarbonothioylthio)-2-methylpropanoic acid (32 mg, 0.088 mmol), and *N*-hydroxyethyl acrylamide (1 g, 8.8 mmol) were dissolved in 1:1 methanol/toluene (4 mL) in a glass vial containing a stir bar. The reaction mixture was degassed under a flow of nitrogen for 10 min, sealed then heated at 70 °C for 30 min. The reaction mixture was opened to air and quenched in liquid nitrogen. The polymer was precipitated into diethyl ether to give a light yellow solid. ^{1}H NMR (400 MHz, D-MeOH): δ 4.79−4.94 (br s, CONH-CH_2-CH_2-OH), 3.58−3.80 (br s, CONH-CH_2-CH$_2$-OH), 3.07−3.23 (br s, CONH-CH_2-CH$_2$-OH), 1.36−2.32 (br, polymer backbone). M_n^{SEC}(THF) = 4900 g·mol^{-1}; M_w/M_n (SEC) = 1.12.

RESULTS AND DISCUSSION

Previous reports on the role of PVA on ice nucleation have been in vitrified solutions (i.e., containing >20% of an organic cosolvent) and using poorly defined materials with broad molecular weight distributions and variable degrees of acetate hydrolysis (as is found in most commercial samples). Our previous work on the impact of synthetic polymers on ice crystal growth (again, not to be confused with nucleation) has shown that both molecular weight and degree of hydrolysis are crucial parameters in their activity.[25] Therefore, a RAFT/MADIX methodology was employed in order to access well-defined polymers such that the effect of polymer chain size could be reliably interrogated. Using a xanthate chain transfer agent (Scheme 1), the molecular weight of the polymer can be tuned by controlling the monomer to initiator ratio. Following polymerization and isolation, the polymers were characterized by ^{1}H NMR and SEC, the results are shown in Table 1, and example SEC traces are shown in Figure 1. All the reactions were conducted in bulk, which has been shown to be an efficient method to polymerize vinyl acetate in a controlled fashion when the ratio of monomer to chain transfer agent is around 100−200. Short chain oligomers of PVAc were prepared by quenching the reaction at low conversion. Using this strategy, well-defined polymers were obtained with dispersity values ($Đ$ = M_w/M_n) below 1.5 (which is expected for deactivated monomers such as VAc, especially at higher [M]/[CTA] ratios) and molecular weights close to that predicted by the feed ratio. The obtained PVAc polymers were hydrolyzed using hydrazine hydrate solution, which gives

DOI: 10.1021/acs.biomac.5b00774
Biomacromolecules 2015, 16, 2820−2826

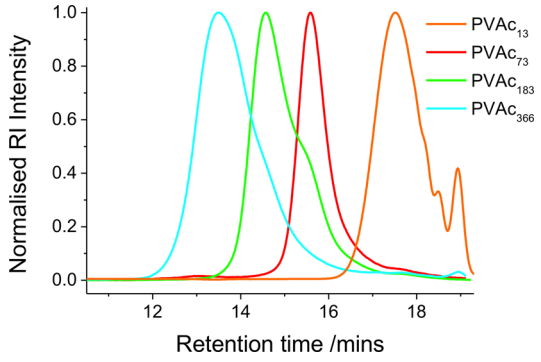

Figure 1. Size exclusion chromatography (SEC) traces of polymers. The low molecular weight shoulder seen in $PVAc_{183}$ can be attributed to termination via chain transfer.

quantitative deprotection, unlike saponification with KOH or NaOH, as we have previously reported.[41]

A key aim of this study is to study the underlying structural features of synthetic polymers, which enable ice nucleation inhibition. Therefore, a panel of other water-soluble, synthetic polymers, poly(hydroxyethyl acrylamide) (pHEA), poly(*N*-isopropylacrylamide) (pNIPAM), and poly((oligo ethylene glyco)methacrylate (pOEGMA), were prepared by RAFT/MADIX polymerization. (Table 2). In all cases well-defined polymers were obtained, except for pOEGMA, which gave a larger than expected dispersity which was thought to be due to column-interactions in the SEC analysis. This dispersity, in this case, does not affect the later discussion (see below).

Ice nucleation is a stochastic process; essentially this means that, in sufficiently small samples (to reduce the number of unwanted nucleators), the temperature of freezing will always vary and therefore single-point measurements do not give reliable nor useful data, such as that from bulk DSC (differential scanning calorimetry) freezing measurements.[42] To reduce these effects, a droplet freezing assay, was employed.[9] Briefly, very small volume (0.5 μL) droplets of ultrapure (Milli-Q) water were added to a hydrophobic glass slide. Small droplets reduce the probability of competing nucleators being present and enable a true "average" nucleation temperature to be determined. These droplets were cooled on a cryostage, under an atmosphere of dry nitrogen, and the freezing point of each droplet recorded by visual observation using a microscope. An example is shown in Figure 2. Differential ice nucleation plots can then be obtained by recording the percentage of droplets frozen versus freezing temperature.

Using the multipoint freezing assay, concentrated (10 mg·mL^{-1}) PVA solutions were prepared and evaluated. Differential ice nucleation plots are shown in Figure 3A, and the temperature at which 50% of all the droplets were frozen for each sample are displayed in Figure 3B to facilitate comparison.

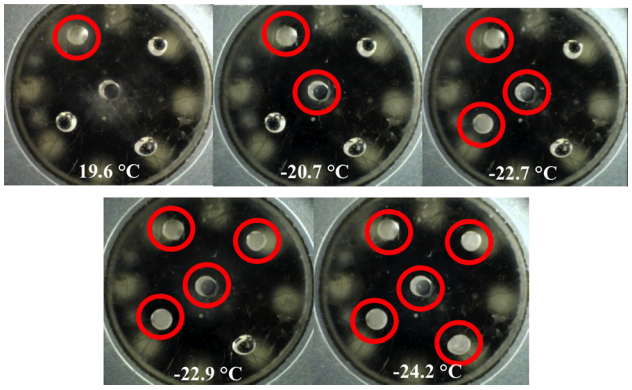

Figure 2. Pictures of the multipoint freezing assay. Nucleating droplets are circled in red, the concentric ring is the reflection of the microscope LEDs.

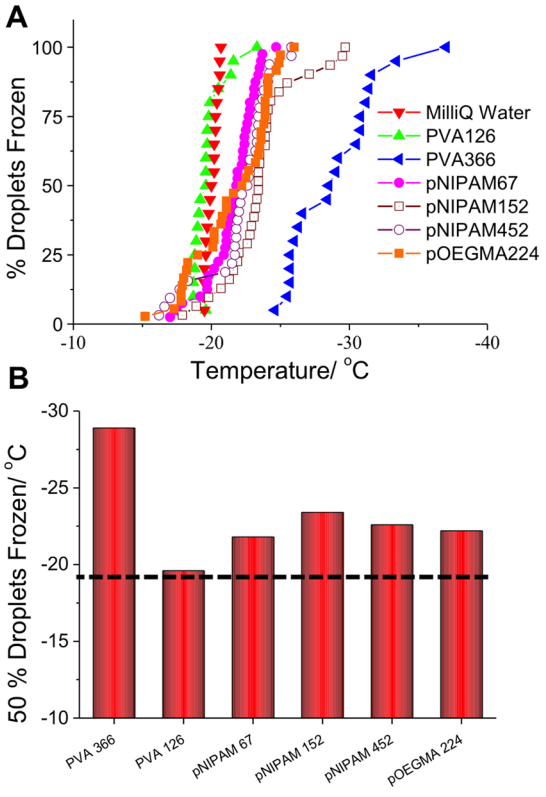

Figure 3. Ice nucleation measurements activity of polymers at 10 mg·mL^{-1} of polymer in solution. (A) Differential ice nucleation plots; (B) Temperature at which 50% of the droplets were frozen, for each polymer sample (no error bars shown to prevent confusion between error and the stochastic processes). Dotted line is to guide the eye toward nucleation temperature of Milli-Q water.

Table 2. Polymers Prepared for Use in This Study

entry	[M]/[CTA]	conv.[a]	M_n(NMR)[a] [g mol^{-1}]	M_n(SEC)[b] [g mol^{-1}]	$Đ$[b]	DP_n[a]
$p(NIPAM)_{67}$	75	88.8	7500	9280	1.05	67
$p(NIPAM)_{152}$	600	25.3	17000	15500	1.27	152
$p(NIPAM)_{452}$	600	75.4	51000	55900	1.12	452
$p(OEGMA)_{224}$	650	34.4	67100	175749	1.92	224
$pHEA_{83}$	100	83.0	9900	10000[c]	1.17	83

[a]Determined from conversion of monomer to polymer by ^{1}H NMR. [b]Determined by SEC in THF using PMMA polymer standards. [c]Determined by SEC in DMF (inc. 5 mM NH_3BF_4) relative to PMMA standards.

DOI: 10.1021/acs.biomac.5b00774
Biomacromolecules 2015, 16, 2820−2826

The other polymers in Table 2 were also tested using this methodology.

In line with previous reports using highly disperse PVA, some inhibition was observed relative to that of the water sample alone (−19 °C, see Figure 4). A very short PVA

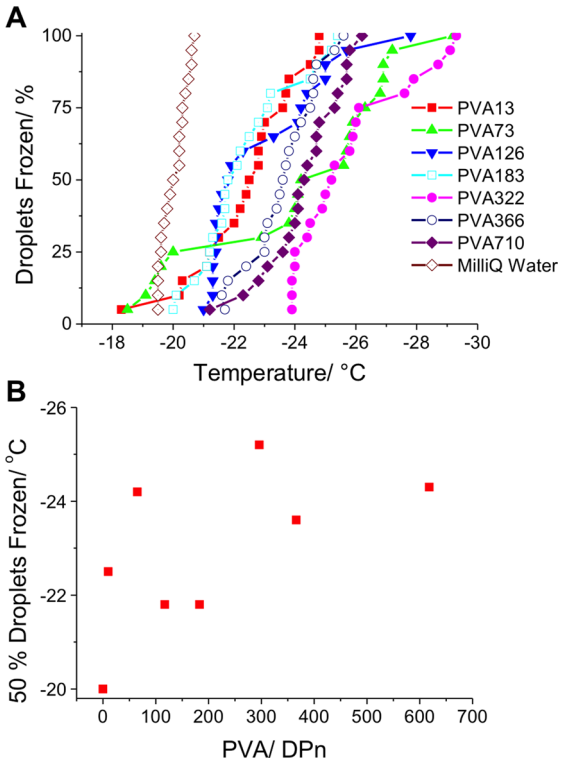

Figure 4. Ice nucleation inhibition activity of RAFT/MADIX synthesized PVA. All assays were run using a concentration of 1 mg·mL^{-1} of polymer in solution. (A) Differential ice nucleation plots; (B) Temperature at which 50% of the droplets were frozen for each PVA sample (no error bars shown to prevent confusion between error and the stochastic process). DP = number-average degree of polymerization.

(PVA13) was tested but gave inconsistent results at these concentrations; purification of short polymers by dialysis is not possible, which may explain this observation. Also, at equal mass concentration, the molar concentration of the short polymer is significantly larger, which we cannot rule out playing a role. Lower concentration data is included later in this paper. The longest chain tested (DP = 366) depressed the temperature to −29 °C. This is a remarkable shift in nucleation and considering the total mass of polymer (and, hence, [OH]) was constant (compared to shorted polymers), this suggests a complex mechanism of interaction to promote this inhibition. We have previously observed similar trends in the ice-growth inhibition activity of PVA, but we believe these are mechanistically unrelated.[25,43] To rule out viscosity as the reason for this behavior, the pNIPAM and pOEGMA polymers (with high molecular weights) were also tested. These all displayed similar freezing point depression irrespective of molecular weight or functionality. In fact, both these polymers gave droplet freezing points of around −23 °C, which is lower than Milli-Q water, which displays a nucleation temperature in the range of −19 °C.[44] Clearly, the activity of PVA is rather unique, even though some activity was observed here with the other polymers. These results mirror observations in ice recrystallization inhibition assays, where the activity of PVA has been shown to be strongly weight (M_n) dependent. To investigate this further, a larger number of PVAs were tested, but with a lowering of the concentration to 1 mg·mL^{-1} to enable any concentration-dependent effects to be separated but also to ensure it is predictive of any applications (i.e., biomedical) where lower concentrations are desirable, Figure 4.

Figure 4 shows that even at 1 mg·mL^{-1} concentration the longer PVAs still had significant ice nucleation inhibition activity. The trend was not linear, potentially as a result of the inherent dispersity of the polymers and the stochastic nature of the assays employed here. Nonetheless this observation confirms that macromolecular engineering of PVA enables the magnitude of the inhibition activity to be controlled, and presents a new tool toward predictable and controllable nucleation.

The results shown above confirm that molecular weight and the structure of PVA relative to other synthetic polymers both contribute to its activity. However, the control polymers used above (pNIPAM and pOEGMA) do not contain hydroxyl groups in their side chain. A simplistic consideration of the possible mechanisms of nucleation inhibition could involve hydrogen bond formation between ice nuclei and the polymers, meaning that other poly(hydroxylated) macromolecules should also be tested. Therefore, $pHEA_{83}$ and also the polysaccharide dextran (9−10 kDa) were tested at 10 mg·mL^{-1} (to ensure effects are pronounced) and the results are shown in Figure 5.

Figure 5 shows that high molecular weight PVA is more effective at depressing the freezing point of water compared to other poly ols at a similar concentration. PVA_{126} (M_n = 5550 g·

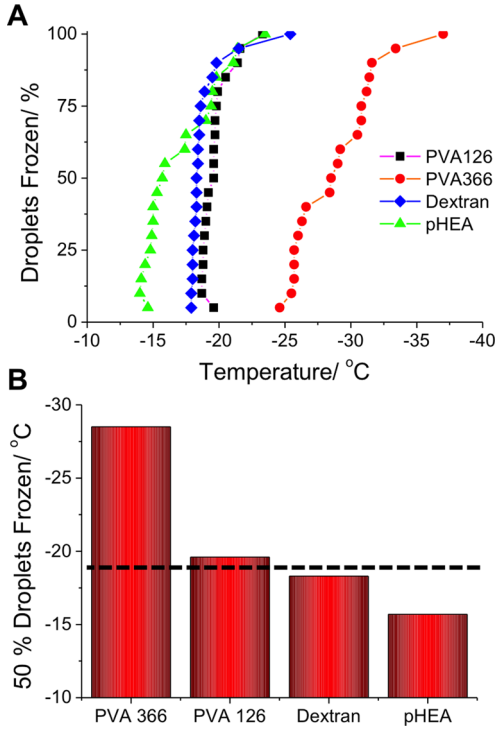

Figure 5. Ice nucleation inhibition activity of PVA, pHEA, and dextran. All assays were run using a concentration of 10 mg·mL^{-1} of polymer in solution. (A) Differential ice nucleation plots; (B) Temperature at which 50% of droplets were frozen for each sample (no error bars shown to prevent confusion between error and stochastic processes).

DOI: 10.1021/acs.biomac.5b00774
Biomacromolecules 2015, 16, 2820−2826

mol^{-1}) shows no activity, similar to Dextran (MW = 9000−10000) and pHEA (M_n = 9900), despite its comparatively low molecular weight, suggesting that this behavior in part arises from a property intrinsic to PVA. Although the pHEA samples do slightly lower the nucleation temperature, we are not willing to claim it is strongly promoting this, but may warrant further study. Classical nucleation theory suggests that nucleation probability decreases with solution viscosity, which can explain molecular weight trends, but not the underlying activity seen here. The reasons for the inhibition properties of these polymers remains unclear; the polymers may be directly interacting with the small ice nuclei that form, inhibiting them, or by blocking the activity of other ice nucleators in solution. There is precedent both of these phenomena. For example, PVP and poly(caprolactam)s are capable of inhibiting the formation of methane hydrate crystals[45] in gas pipelines by directly interacting with and disrupting the formation when the crystals have just nucleated and begun to crystallize.[46,47]

However, considering the body of evidence showing how polymers and proteins nullify ice nucleators, this may be the more likely of the two mechanisms. Wowk and Fahy observed polymers interacting with nucleating agents; polyglycerol was found to bind and inhibit the ice nucleation activity of some proteins, and the combination of polyglycerol with poly(vinyl alcohol) was shown to be particularly effective for reducing ice formation in vitrified solutions.[26] Inada et al. have demonstrated that PVA is very effective at blocking silver iodide induced ice nucleation, which is hypothesized to be due to it binding to the surface of the AgI nucleators.[48,49] PVA has also been shown to deactivate the nucleating ability of the ice nucleating proteins from *Pseudomonas syringae*.[16] In contrast to these reports, our assay made every attempt to exclude nucleators, but from the freezing point of around −20 °C observed for Milli-Q, here it appears that heterogeneous nucleation still dominates, even with the high purity water. The fact that PVA solutions display a depressed ice nucleation temperature, taken with the above reports, lead us to believe that PVA is interacting with whatever nucleators exist in Milli-Q water, but we cannot rule out direct interaction with the ice nuclei.

For in vivo application, the polymer must either be degradable (which PVA is not in the human body) or sufficiently small that it can be excreted by glomerular filtration, while maintaining activity. It is interesting to observe here that longer polymers are also more active at inhibition, although a mechanism is not yet presented. Conversely, we have previously shown that PVA with just a DP of 20 is required for significant ice recrystallization (growth) inhibition, implying that these related, but separate, processes may have different structural requirements. The results shown here suggest that, in addition to the chemical composition, the macromolecular architecture of polymers can hugely influence ice nucleation properties and offers a synthetically accessible tool for probing this most fundamental, but misunderstood (often conflated with freezing point depression or ice growth), process. Identifying the molecular weight of the polymers that are most efficient is also crucial in the development of these for biomedical applications. Future work will focus not only on understanding the INI activity of these and other synthetic polymers, but their ability to influence the heterogeneous as well as homogeneous nucleation and how this links with their other known "antifreeze" properties of thermal hysteresis (freezing point depression) and ice recrystallization inhibition.

CONCLUSIONS

Here, the ice nucleation inhibition activity of poly(vinyl alcohol) has been studied in detail. RAFT/MADIX polymerization was employed to access polymers with predictable molecular weights and low dispersity (M_w/M_n) values. Using differential ice nucleation analysis, the heterogeneous nucleation temperature of the "pure" water used here was determined to be −19 °C. The well-defined polymers revealed a significant molecular weight dependent ice nucleation inhibition effect, with the shortest polymers decreasing nucleation by only 2 °C, but the longest by almost 10 °C. These preliminary findings show that, in addition to affecting ice crystal growth, PVA also has the unique effect of inhibiting ice nucleation, which may provide insight into this complex process, controlled by seemingly simple polymers. Furthermore, this work shows that polymer architecture may also be used as a tool to modulate ice nucleation activity. These polymers will enable us to study the unique ice nucleation process in detail, and the results help to design new macromolecular tools for extreme-cold environments.

ASSOCIATED CONTENT

Supporting Information

Details on the synthesis of both RAFT agents and the conversion of PVAc to PVA. The Supporting Information is available free of charge on the ACS Publications website at DOI: 10.1021/acs.biomac.5b00774.

(PDF)

AUTHOR INFORMATION

Corresponding Author

*Fax: +44 247 652 4112. E-mail: m.i.gibson@warwick.ac.uk.

Notes

The authors declare no competing financial interest.

ACKNOWLEDGMENTS

The Leverhulme Trust are thanked for funding for a studentship to T.C. via the Research Grant RPG-144. The University of Warwick is thanked for providing undergraduate bursaries (URSS and via the Materials Global Research Priority) for B.D. The cryostage used here was purchased with support from a research grant from the Royal Society, U.K. Equipment used was supported by the Innovative Uses for Advanced Materials in the Modern World (AM2), with support from Advantage West Midlands (AWM) and part funded by the European Regional Development Fund (ERDF). C.I.M. is funded by BBSRC Life Science Doctoral Training Partnership. M.I.G. acknowledges the ERC for a starter grant (CRYOMAT 638661).

REFERENCES

(1) Abbatt, J. P. D. *Chem. Rev.* **2003**, *103*, 4783−4800.
(2) John Morris, G.; Acton, E. *Cryobiology* **2013**, *66*, 85−92.
(3) Fowler, A.; Toner, M. *Ann. N. Y. Acad. Sci.* **2005**, *1066*, 119−135.
(4) Rubinsky, B. *Annu. Rev. Biomed. Eng.* **2000**, *2*, 157−187.
(5) Petzold, G.; Aguilera, J. *Food Biophys.* **2009**, *4*, 378−396.
(6) Wowk, B. *Cryobiology* **2010**, *60*, 11−22.
(7) Damodaran, S. *J. Agric. Food Chem.* **2007**, *55*, 10918−10923.
(8) Murray, B. J.; Broadley, S. L.; Wilson, T. W.; Atkinson, J. D.; Wills, R. H. *Atmos. Chem. Phys.* **2011**, *11*, 4191−4207.

DOI: 10.1021/acs.biomac.5b00774
Biomacromolecules 2015, 16, 2820−2826

(9) Atkinson, J. D.; Murray, B. J.; Woodhouse, M. T.; Whale, T. F.; Baustian, K. J.; Carslaw, K. S.; Dobbie, S.; O'Sullivan, D.; Malkin, T. L. *Nature* **2013**, *498*, 355.
(10) Murray, B. J.; O'Sullivan, D.; Atkinson, J. D.; Webb, M. E. *Chem. Soc. Rev.* **2012**, *41*, 6519−6554.
(11) Duman, J. G. *Annu. Rev. Physiol.* **2001**, *63*, 327−357.
(12) Kawahara, H. *J. Biosci. Bioeng.* **2002**, *94*, 492−496.
(13) Cochet, N.; Widehem, P. *Appl. Microbiol. Biotechnol.* **2000**, *54*, 153−161.
(14) Wilson, P. W.; Leader, J. P. *Biophys. J.* **1995**, *68*, 2098−2107.
(15) Gurian-Sherman, D.; Lindow, S. E. *FASEB J.* **1993**, *7*, 1338−1343.
(16) Holt, C. B. *CryoLetters* **2003**, *24*, 323−330.
(17) Eto, T. K.; Rubinsky, B. *Biochem. Biophys. Res. Commun.* **1993**, *197*, 927−931.
(18) Wilson, P. W.; Osterday, K. E.; Heneghan, A. F.; Haymet, A. D. J. *J. Biol. Chem.* **2010**, *285*, 34741−34745.
(19) Zachariassen, K. E.; Kristiansen, E. *Cryobiology* **2000**, *41*, 257−279.
(20) Parody-Morreale, A.; Murphy, K. P.; Di Cera, E.; Fall, R.; DeVries, A. L.; Gill, S. J. *Nature* **1988**, *333*, 782−783.
(21) Wilkinson, B. L.; Stone, R. S.; Capicciotti, C. J.; Thaysen-Andersen, M.; Matthews, J. M.; Packer, N. H.; Ben, R. N.; Payne, R. J. *Angew. Chem., Int. Ed.* **2012**, *51*, 3606−3610.
(22) Trant, J. F.; Biggs, R. A.; Capicciotti, C. J.; Ben, R. N. *RSC Adv.* **2013**, *3*, 26005−26009.
(23) Gibson, M. I. *Polym. Chem.* **2010**, *1*, 1141−1152.
(24) Deller, R. C.; Congdon, T.; Sahid, M. A.; Morgan, M.; Vatish, M.; Mitchell, D. A.; Notman, R.; Gibson, M. I. *Biomater. Sci.* **2013**, *1*, 478−485.
(25) Congdon, T.; Notman, R.; Gibson, M. I. *Biomacromolecules* **2013**, *14*, 1578−1586.
(26) Wowk, B.; Fahy, G. M. *Cryobiology* **2002**, *44*, 14−23.
(27) Franks, F.; Darlington, J.; Schenz, T.; Mathias, S. F.; Slade, L.; Levine, H. *Nature* **1987**, *325*, 146−147.
(28) Inada, T.; Modak, P. R. *Chem. Eng. Sci.* **2006**, *61*, 3149.
(29) Wang, H.-Y.; Inada, T.; Funakoshi, K.; Lu, S.-S. *Cryobiology* **2009**, *59*, 83−89.
(30) Stan, C. A.; Schneider, G. F.; Shevkoplyas, S. S.; Hashimoto, M.; Ibanescu, M.; Wiley, B. J.; Whitesides, G. M. *Lab Chip* **2009**, *9*, 2293−2305.
(31) Butorin, G. T.; Skripov, V. P. *Kristallografiya* **1972**, *17*, 379.
(32) Krämer, B.; Hübner, O.; Vortisch, H.; Wöste, L.; Leisner, T.; Schwell, M.; Rühl, E.; Baumgärtel, H. *J. Chem. Phys.* **1999**, *111*, 6521−6527.
(33) Duft, D.; Leisner, T. *Atmos. Chem. Phys.* **2004**, *4*, 1997−2000.
(34) Murray, B. J.; Broadley, S. L.; Wilson, T. W.; Bull, S. J.; Wills, R. H.; Christenson, H. K.; Murray, E. J. *Phys. Chem. Chem. Phys.* **2010**, *12*, 10380−10387.
(35) Campbell, J. M.; Meldrum, F. C.; Christenson, H. K. *J. Phys. Chem. C* **2015**, *119*, 1164−1169.
(36) Ogawa, S.; Koga, M.; Osanai, S. *Chem. Phys. Lett.* **2009**, *480*, 86−89.
(37) Inada, T.; Koyama, T.; Goto, F.; Seto, T. *J. Phys. Chem. B* **2011**, *115*, 7914−7922.
(38) Skey, J.; O'Reilly, R. K. *Chem. Commun.* **2008**, 4183−4185.
(39) Wilkins, L. E.; Phillips, D. J.; Deller, R. C.; Davies, G.-L.; Gibson, M. I. *Carbohydr. Res.* **2015**, *405*, 47−54.
(40) Phillips, D. J.; Gibson, M. I. *Biomacromolecules* **2012**, *13*, 3200−3208.
(41) Congdon, T.; Shaw, P.; Gibson, M. I. *Polym. Chem.* **2015**, *6*, 4749−4757.
(42) Niedermeier, D.; Shaw, R. A.; Hartmann, S.; Wex, H.; Clauss, T.; Voigtländer, J.; Stratmann, F. *Atmos. Chem. Phys.* **2011**, *11*, 8767−8775.
(43) Inada, T.; Lu, S. S. *Cryst. Growth Des.* **2003**, *3*, 747−752.
(44) O'Sullivan, D.; Murray, B. J.; Ross, J. F.; Whale, T. F.; Price, H. C.; Atkinson, J. D.; Umo, N. S.; Webb, M. E. *Sci. Rep.* **2015**, *5*, 8082.
(45) O'Reilly, R.; Ieong, N. S.; Chua, P. C.; Kelland, M. A. *Energy Fuels* **2011**, *25*, 4595−4599.
(46) Storr, M. T.; Taylor, P. C.; Monfort, J.-P.; Rodger, P. M. *J. Am. Chem. Soc.* **2004**, *126*, 1569−1576.
(47) Kelland, M. A. *Energy Fuels* **2006**, *20*, 825−847.
(48) Koyama, T.; Inada, T.; Kuwabara, C.; Arakawa, K.; Fujikawa, S. *Cryobiology* **2014**, *69*, 223−228.
(49) Inada, T.; Koyama, T.; Goto, F.; Seto, T. *J. Phys. Chem. B* **2012**, *116*, 5364−5371.

DOI: 10.1021/acs.biomac.5b00774
Biomacromolecules 2015, 16, 2820−2826